# Zinc Finger–DNA Recognition: Crystal Structure of a Zif268-DNA Complex at 2.1 Å

NIKOLA P. PAVLETICH AND CARL O. PABO

**The zinc finger DNA-binding motif occurs in many proteins that regulate eukaryotic gene expression. The crystal structure of a complex containing the three zinc fingers from Zif268 (a mouse immediate early protein) and a consensus DNA-binding site has been determined at 2.1 angstroms resolution and refined to a crystallographic *R* factor of 18.2 percent. In this complex, the zinc fingers bind in the major groove of B-DNA and wrap partway around the double helix. Each finger has a similar relation to the DNA and makes its primary contacts in a three–base pair subsite. Residues from the amino-terminal portion of an α helix contact the bases, and most of the contacts are made with the guanine-rich strand of the DNA. This structure provides a framework for understanding how zinc fingers recognize DNA and suggests that this motif may provide a useful basis for the design of novel DNA-binding proteins.**

THE ZINC FINGER IS ONE OF THE MAJOR STRUCTURAL motifs involved in eukaryotic protein–nucleic acid interactions. The fingers that were first discovered in the *Xenopus* transcription factor IIIA (TFIIIA) (*1*) contain a sequence motif of the form $X_3$-Cys-$X_{2-4}$-Cys-$X_{12}$-His-$X_{3-4}$-His-$X_4$ (where X is any amino acid), and hundreds of similar finger sequences have been reported (*2*). Only a few of the proteins that contain such fingers have been studied in detail, but it appears that many of these zinc finger domains are involved in DNA binding. Proteins with zinc finger domains are involved in many aspects of eukaryotic gene regulation. For example, such fingers occur in proteins induced by differentiation and growth signals [EGR1 (*3, 4*), EGR2 (*5, 6*)], in proto-oncogenes [GLI (*7*), Wilms' tumor gene (*8*)], in general transcription factors [Sp1 (*9*)], in *Drosophila* segmentation genes [*Hunchback* (*10*), *Kruppel* (*11*)], and in regulatory genes of lower eukaryotic organisms [*ADR1* (*12*), *BrlA* (*13*)]. The term zinc finger has been used in many different ways, and therefore it is important to realize that the characteristic sequence patterns and the three-dimensional structures of the TFIIIA-like zinc fingers are distinct from those of the cysteine-rich motifs in the steroid receptors (*14*), the cysteine-rich motif in the yeast transcription factor GAL4 (*15*), or the Cys-Cys-His-Cys motif in a set of retroviral proteins (*16*). In our study, we have focused on zinc fingers that are homologous to the fingers in TFIIIA.

Recent NMR (nuclear magnetic resonance) studies (*17, 18*) have shown that the TFIIIA-like zinc fingers contain an antiparallel β ribbon and an α helix. The two invariant cysteines, which are near the turn in the β-ribbon region, and the two invariant histidines, which are in the COOH-terminal portion of the α helix, coordinate a central zinc ion, and the finger forms a compact globular domain. There has been no structural information about how individual fingers interact with the DNA, or how proteins with tandemly repeated fingers recognize their binding sites. Sequence comparisons and mutational analyses have been used to propose a model for the zinc finger–DNA interactions (*19*), but no crystal structures or NMR studies of complexes have been reported.

To understand how these zinc finger domains are used in site-specific recognition, we have expressed and purified a peptide that contains the DNA-binding domain from the mouse immediate early protein Zif268 (*4*) (also known as Krox-24, NGFI-A, and Egr1). We have crystallized this three–zinc finger peptide with a Zif268 consensus binding site (*20*), solved the structure of this complex at 2.1 Å resolution, and refined it to an *R* factor of 18.2 percent. Here we report the structure of the complex, discuss the implications for our understanding of zinc finger–DNA interactions and protein-DNA recognition, and consider the prospect of using zinc finger motifs as a basis for designing novel DNA-binding proteins.

**Cloning and purification of the Zif268–zinc finger peptide.** The portion of the *zif268* cDNA that codes for the three zinc fingers, corresponding to residues 349 to 421 of Zif268 (*4*) (Fig. 1A), was amplified in a polymerase chain reaction (PCR). One of the PCR primers introduced an Nde I restriction enzyme site with an in-frame ATG start codon at the 5′ end of the zinc finger domain (a silent mutation that eliminated a second Nde I site was also introduced). The second PCR primer introduced a TAG stop codon, and a Bam HI restriction enzyme site at the 3′ end. The amplified DNA was cloned into the Nde I and Bam HI sites of the

N. P. Pavletich and C. O. Pabo are in the Department of Molecular Biology and Genetics, Johns Hopkins University School of Medicine, Baltimore, MD 21205. C. O. Pabo also is in the Howard Hughes Medical Institute. The mailing address for both authors after 1 July 1991 is Department of Biology, Massachusetts Institute of Technology, 77 Massachusetts Avenue, Cambridge, MA 02139.

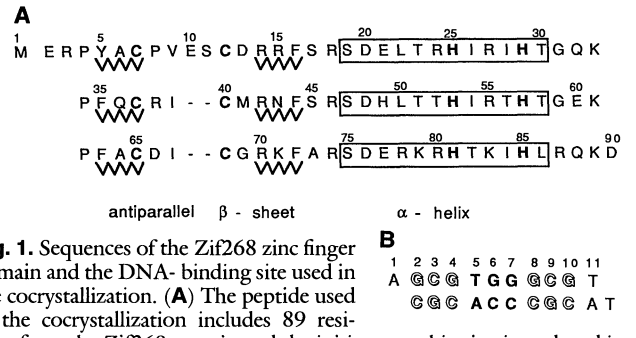


**Fig. 1.** Sequences of the Zif268 zinc finger domain and the DNA- binding site used in the cocrystallization. (**A**) The peptide used in the cocrystallization includes 89 residues from the Zif268 protein and the initiator methionine introduced in the cloning. Only residues 3 to 87 are present in the current model. (We presume that the terminal residues are disordered in the crystal.) The three zinc fingers are aligned to show the conserved residues and secondary structures. Helices are boxed, and the β sheets are indicated by zig-zag lines. The approximate positions for these regions of secondary structure could have been predicted from NMR studies of related zinc fingers; the precise positions were determined from our crystal structure. (**B**) DNA duplex used for cocrystallization. The subsites that the fingers bind to are either in shadowed or in bold letters. These alternate to highlight the 3-bp subsites recognized by the zinc fingers.

pET3a (*21*) expression plasmid and then sequenced. The resulting plasmid (pzif89) was used to transform the *Escherichia coli* strain BL21(D3) that also contained the pLysE plasmid (*21*). Cultures were grown and induced as described (*21*), except that the induction was continued for 18 hours. After the cells were harvested, the *E. coli* pellet was resuspended in a buffer of 25 mM Hepes, pH 7.9, 1 mM EDTA, 100 mM NaCl, 1 mM phenylmethylsulfonyl fluoride (PMSF), and 10 mM dithiothreitol (DTT); the cells were lysed by the addition of NP-40 detergent to a final concentration of 0.2 percent, and the resulting solution was stirred at 4°C for 40 minutes in the presence of 6 mM $MgCl_2$ and deoxyribonuclease I (DNase I) at 65 U/ml. The insoluble inclusion bodies that contained the Zif268–zinc finger peptide were harvested by centrifugation, dissolved in a solution of 6.4 M guanidinium-HCl and 50 mM tris, pH 7.4, and reduced with 150 mM DTT at 75°C for 30 minutes. The peptide was extracted from the solution in batch mode with the use of C4 reversed-phase resin (Vydac), was eluted with 40 percent $CH_3CN$ and 0.1 percent trifluoroacetic acid (TFA), and was lyophilized. The reduction reaction was repeated, and the peptide was purified by chromatography as follows. (i) The peptide was purified on a C4 reversed-phase (Vydac) high-performance liquid chromatography (HPLC) column in 0.1 percent TFA, with a $CH_3CN$ gradient. (ii) The peptide was reconstituted with zinc in a buffer of 50 mM 2-[*N*-morpholino]ethanesulfonic acid–$Na^+$, pH 6.2, and 2 mM DTT, and purified on a MonoS cation exchange column (Pharmacia) with a NaCl gradient. (iii) The peptide was loaded onto a C4 reversed phase HPLC column in 0.1 percent TFA, and eluted with a shallow $CH_3CN$ gradient. The HPLC peak fractions were alternately resuspended in water and lyophilized three times to remove the excess TFA, and the final dried product was stored in an anaerobic chamber (Coy Laboratory Products), where the oxygen content was kept below 1 part per million. The identity of the peptide was confirmed by analysis of amino acid composition. Mobility shift experiments showed that the Zif268–zinc finger peptide binds specifically to the consensus DNA sequence shown in Fig. 1B, with a dissociation constant ($K_d$) of 6 nM (*22*).

**Crystallization and structure determination**. The Zif268–zinc finger peptide–DNA complex (Zif complex) was prepared by adding 1.5 molar equivalents of cobalt chloride or zinc chloride to the apopeptide, adjusting the pH to 8.0, adding 1 molar equivalent of the buffered DNA-binding site, and solubilizing the complex by the addition of NaCl. Cocrystals were grown in the anaerobic chamber by the hanging drop vapor diffusion method. The best crystals were obtained by mixing a 1 mM solution of the complex (in 450 to 750 mM NaCl, 125 mM bis-tris propane-HCl, pH 8.0) with an equal volume of the buffer used in the crystallization well (0.0 to 10.0 percent polyethylene glycol (PEG) 400, 350 to 650 mM NaCl, and 25 mM bis-tris propane-HCl, pH 8.0); the crystals grew over the course of 2 weeks. The crystals form in the space group $C222_1$ with $a$ = 45.4 Å, $b$ = 56.2 Å, and $c$ = 130.8 Å, and have one complex in the asymmetric unit.

Diffraction data were collected with the Siemens area detector (Table 1). Isomorphous derivatives were obtained by preparing duplex DNA in which 5-iodouracil was substituted for thymine at specific positions (at base pair 5 on the upper strand for $IdU^5$, and at the 5′ end of the lower strand for $IdU^{12}$). The structure was first solved and refined with data from crystals of the peptide-$Co^{2+}$-DNA complex. For our final structure, high-resolution data were collected with crystals of the peptide-$Zn^{2+}$-DNA complex at the Midwest Area Detector User Facility. The structure has been refined against these data, and we see no significant differences between the $Zn^{2+}$ and the $Co^{2+}$ structures.

Heavy-atom parameters were first refined with the use of the program REFINE from the CCP4 (*23*) package of crystallographic programs. These data were used to determine initial multiple isomorphous replacement (MIR) phases at 2.5 Å resolution, and phasing with the program PHARE (from the CCP4 package) gave a mean figure of merit of 0.61. After solvent flattening [Wang's protocol (*24*)] this MIR map had very good density for the entire complex. The map was further improved by refining the heavy atom parameters against the solvent-flattened phases (*25*). Two additional cycles of phasing, solvent flattening, and parameter refinement were used to calculate the final map. Phases for the last MIR map had a mean figure of merit of 0.62 for data from 20.0 to 2.5 Å, and this MIR map was used with the FRODO (*26*) graphics program to build a model of the complex.

The electron density for each of the three zinc fingers was excellent

**Table 1.** Statistics from the crystallographic analysis.

| Item | Native | Native | $IdU^5$ | $IdU^{12}$ |
|---|---|---|---|---|
| Metal ion | Zinc | Cobalt | Cobalt | Cobalt |
| Resolution (Å) | 2.1 | 2.4 | 2.5 | 2.5 |
| Measured reflections | 34488 | 27330 | 27264 | 25615 |
| Unique reflections | 9458 | 5880 | 5221 | 5320 |
| Data coverage (percent) | 93.4 | 86.8 | 86.5 | 88.0 |
| $R_{sym}$ | 4.81 | 4.44 | 6.67 | 5.39 |
| MIR analysis: | | | | |
| Resolution limits (Å) | | | 20.0-2.5 | 20.0-2.5 |
| Mean isomorphous difference | | | 0.18 | 0.13 |
| Phasing power | | | 1.92 | 2.02 |
| Cullis $R$ factor | | | 0.60 | 0.52 |
| Refinement: | | | | |
| Resolution limits | 7.0-2.1 | | | |
| $R$ factor | 0.182 | | | |
| Reflections with $F > 2\sigma$ | 9047 | | | |
| Total number of atoms | 1290 | | | |
| Water molecules | 129 | | | |
| rms in $B$ values (Å$^2$) | 3.19 | | | |
| rms in bond lengths (Å) | 0.014 | | | |
| rms in bond angles (deg.) | 2.34 | | | |

$R_{sym} = \Sigma_h\Sigma_i|I_{h,i} - I_h|/\Sigma_h\Sigma_i I_{h,i}$, where $I_h$ is the mean intensity of the $i$ observations of reflection $h$. Mean isomorphous difference = $\Sigma|F_{PH} - F_P|/\Sigma F_{PH}$, where $F_{PH}$ and $F_P$ are the derivative and native structure factor amplitudes, respectively. Phasing power = $[(F_{H(calc)}^2)/(F_{PH(obs)} - F_{PH(calc)})^2]^{1/2}$. Cullis $R$ factor = $\Sigma||F_{der} \pm F_{nat}| - F_{H(calc)}|/\Sigma|F_{der} - F_{nat}|$ for centric reflections, where $F_{H(calc)}$ is the calculated heavy atom structure factor. $R$ factor = $\Sigma|F_{obs} - F_{calc}|/\Sigma F_{obs}$. The rms in $B$ values is the rms deviation in temperature factors between bonded atoms. The rms in bond lengths and bond angles is the rms deviation in bond lengths and bond angles from ideal values.

and was fit with the NMR model of the Xfin31 zinc finger (*18*). The linkers that connect neighboring fingers had strong density and were readily added in at this stage. The electron density for the DNA was fit with individual nucleotide bases that were extracted from a model of uniform B-DNA. We built 88 percent of the complex into this MIR map, leaving out residues 1 to 4 and 87 to 90 of the peptide since they did not have clear electron density. Even though all the side chains that made base contacts were well defined in the electron density map, they were omitted in the early stages of refinement in order to minimize model bias.

The model was refined with the program X-PLOR (*27, 28*), which applies molecular dynamics with crystallographic restraints. The first cycle of simulated annealing gave an *R* factor of 27.0 percent for data from 10.0 to 2.5 Å. Simulated annealing was repeated after minor rebuilding and after adding three of the missing residues and all of the critical side chains. The second cycle of simulated annealing refinement gave a model with an *R* factor of 25.0 percent for data from 7.0 to 2.4 Å.

This partially refined structure of the peptide-$Co^{2+}$-DNA complex was used as the starting model for refinement against the high-resolution data from the peptide-$Zn^{2+}$-DNA crystals. We used several additional rounds of simulated annealing, gradually added 129 water molecules, and refined individual temperature factors. In the final stages of refinement, the TNT (*29*) package was used for least squares refinement. The structure presented here has an *R* factor of 18.2 percent for data from 7.0 to 2.1 Å. The root-mean-square (rms) deviation from ideality for bond lengths is 0.014 Å, and the rms deviation for bond angles is 2.34°.

To determine whether the high salt concentration used for cocrystallization perturbed the structure in any way, data were also collected from cobalt cocrystals that had been equilibrated in low ionic strength buffer (about 150 mM NaCl). The low salt structure has been refined to an *R* factor of 23.2 percent for data from 7.0 to 2.2 Å, with individually refined temperature factors. Comparison with the high salt structure does not reveal any significant changes. Thus there is no indication that the high salt in the other crystals affected any key aspects of the structure. The crystals are quite stable at 150 mM NaCl, but higher salt concentrations are required to initially solubilize the complex for crystallization.

**Overall structure of the zinc finger–DNA complex.** The overall structure of the complex reveals why tandemly repeated zinc fingers are such efficient motifs for protein-DNA recognition: the three zinc fingers are arranged in a semicircular (C-shaped) structure that fits snugly into the major groove of B-DNA (Fig. 2). As expected from NMR studies of individual fingers (*17, 18*), each zinc finger domain consists of an antiparallel β sheet and an α helix, held together by a zinc ion and by a set of hydrophobic residues. Two cysteines from the β-sheet region and two histidines from the α helix coordinate the zinc ion.

Our cocrystal structure shows that the α helix of each zinc finger fits directly into the major groove and that residues from the $NH_2$-terminal portion of each α helix contact the base pairs in the major groove. Each of the three Zif268 zinc fingers uses its α helix in a similar fashion, and each finger makes its primary contacts with a 3-bp subsite. The overall structure of the complex exhibits periodicity, with neighboring fingers related in a way that reflects the 3-bp periodicity of the subsites. A rotation of approximately 96° (3 × 32°) around the DNA axis, and a translation of approximately 10 Å (3 × 3.3 Å) along the DNA axis, move one finger onto the next. Although the α helix fits into the major groove, its axis is only approximately aligned with the groove, and the α helix is tipped at a somewhat steeper angle (about 45° with respect to the plane of the base pairs) than the angle of the major groove (32°). The β sheet is on the back of the helix away from the base pairs and is shifted toward one side of the major groove. The two strands of the β sheet have very different roles in the complex. The first β strand does not make any contacts with the DNA, whereas the second β strand contacts the sugar phosphate backbone along one strand of the DNA.

The Zif268–zinc finger peptide makes 11 critical hydrogen bonds with the bases in the major groove. The important side chains include an arginine that immediately precedes the α helix in each of the three fingers and also include the second, the third, and the sixth residues in the α helices. All of these hydrogen bonds involve bases on the G-rich strand of the consensus binding site (5′-GCGTGGGCG-3′). Using the 5′->3′ convention for the direction of a DNA strand and the N->C convention for the direction of a polypeptide strand, we might say that the overall arrangement of the peptide is "antiparallel" to the DNA strand that has most of the contacts. The peptide is arranged so that finger 1 binds near the 3′ end of the primary strand (GCG TGG **GCG**); finger 2 binds near the center (GCG **TGG** GCG); and finger 3 binds near the 5′ end (**GCG** TGG GCG). [(Chemical analysis of the TFIIIA-DNA complex also indicated that most of the contacts involve the guanine-rich strand of the DNA and that the TFIIIA fingers also are "antiparallel" to the G-rich strand (*30, 31*).]

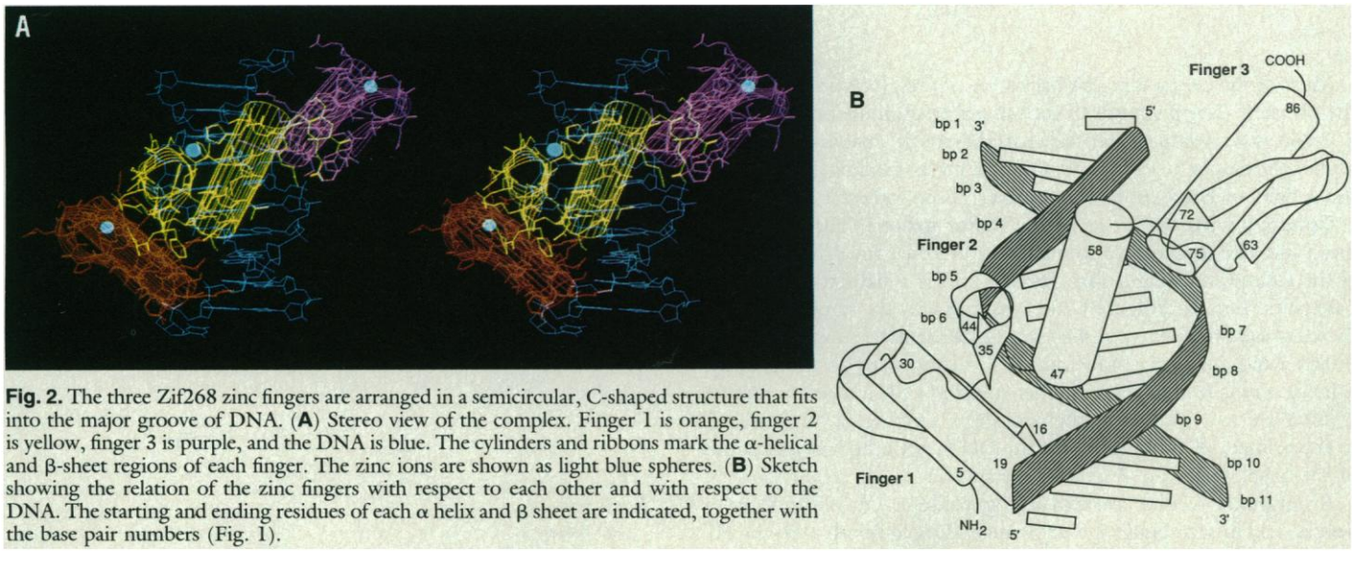


**Fig. 2.** The three Zif268 zinc fingers are arranged in a semicircular, C-shaped structure that fits into the major groove of DNA. (**A**) Stereo view of the complex. Finger 1 is orange, finger 2 is yellow, finger 3 is purple, and the DNA is blue. The cylinders and ribbons mark the α-helical and β-sheet regions of each finger. The zinc ions are shown as light blue spheres. (**B**) Sketch showing the relation of the zinc fingers with respect to each other and with respect to the DNA. The starting and ending residues of each α helix and β sheet are indicated, together with the base pair numbers (Fig. 1).

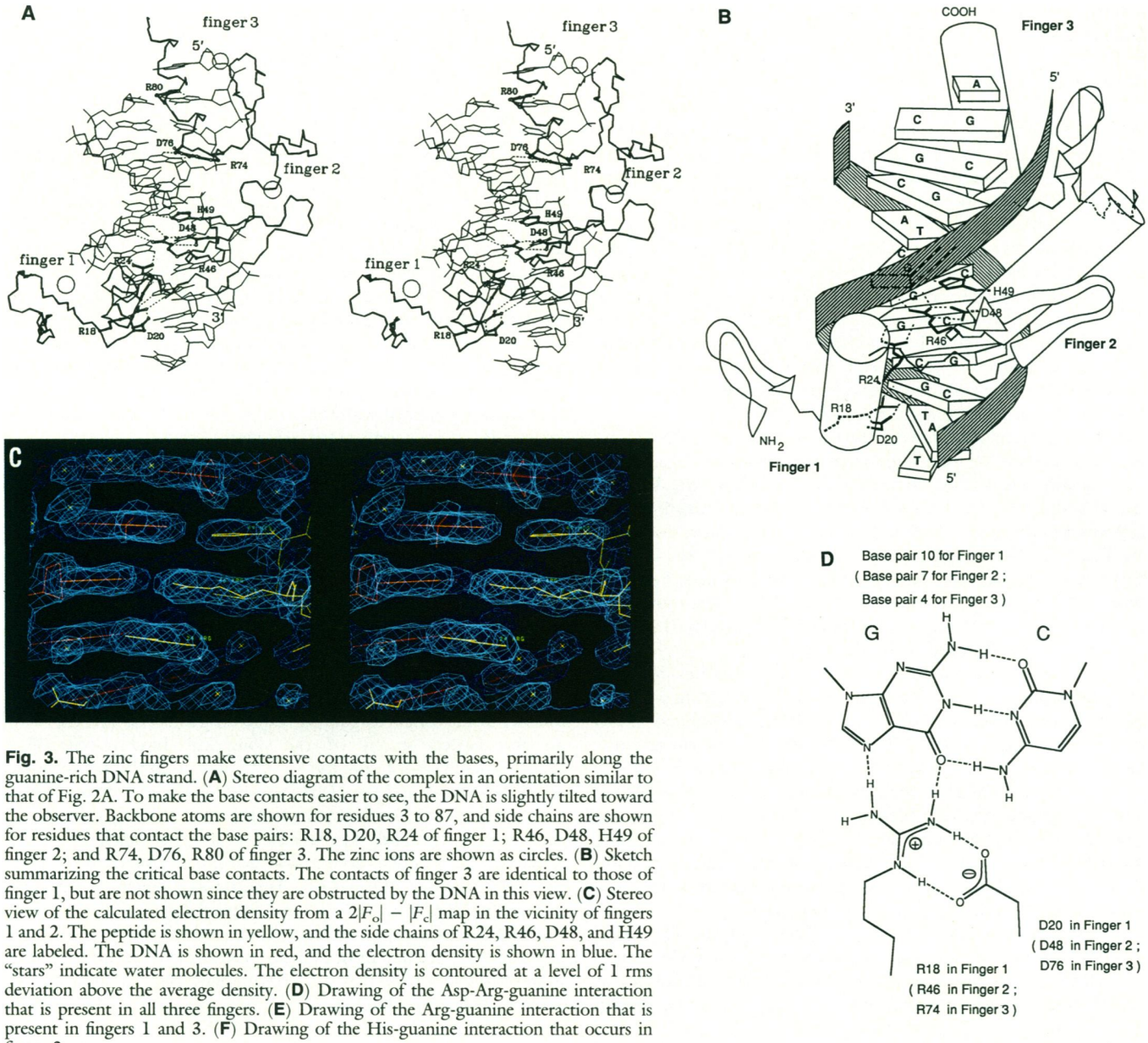


**Fig. 3.** The zinc fingers make extensive contacts with the bases, primarily along the guanine-rich DNA strand. (**A**) Stereo diagram of the complex in an orientation similar to that of Fig. 2A. To make the base contacts easier to see, the DNA is slightly tilted toward the observer. Backbone atoms are shown for residues 3 to 87, and side chains are shown for residues that contact the base pairs: R18, D20, R24 of finger 1; R46, D48, H49 of finger 2; and R74, D76, R80 of finger 3. The zinc ions are shown as circles. (**B**) Sketch summarizing the critical base contacts. The contacts of finger 3 are identical to those of finger 1, but are not shown since they are obstructed by the DNA in this view. (**C**) Stereo view of the calculated electron density from a $2|F_o| - |F_c|$ map in the vicinity of fingers 1 and 2. The peptide is shown in yellow, and the side chains of R24, R46, D48, and H49 are labeled. The DNA is shown in red, and the electron density is shown in blue. The "stars" indicate water molecules. The electron density is contoured at a level of 1 rms deviation above the average density. (**D**) Drawing of the Asp-Arg-guanine interaction that is present in all three fingers. (**E**) Drawing of the Arg-guanine interaction that is present in fingers 1 and 3. (**F**) Drawing of the His-guanine interaction that occurs in finger 2.

Most of the contacts to the backbone of the DNA are made with the primary, G-rich strand. In each finger an arginine on the second β strand (two residues after the second cysteine) makes a contact to a phosphodiester oxygen, and the first metal binding histidine on the α helix makes a contact to another phosphodiester oxygen.

**Contacts with the bases in the major groove.** The zinc finger motif uses the residue that immediately precedes the α helix, as well as the second, third, and sixth residues of the α helix to contact the base pairs (Fig. 3). Fingers 1 and 3 have exactly the same residues at these critical positions, and they recognize identical subsites (GCG). Finger 2 has different residues at the third and sixth positions of the α helix, and it recognizes a distinct subsite (TGG). The orientation of each α helix, like that of the peptide as a whole, is "antiparallel" to the primary (G-rich) strand of the DNA, with the $NH_2$-terminus of the α helix near the 3′ end of the subsite.

An arginine residue immediately precedes each of the three α helices, and in each finger this arginine hydrogen bonds with the N7

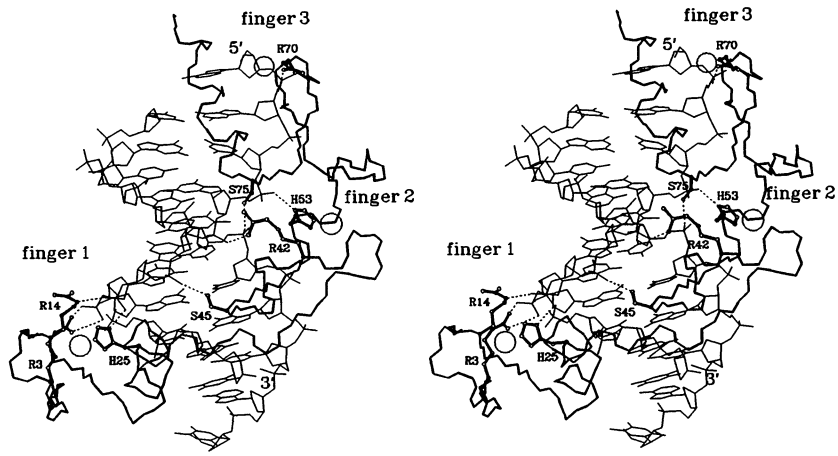


**Fig. 4.** Contacts with the phosphates. Stereo diagram showing the backbone atoms for residues 3 to 87 and the side chains of the residues that contact the phosphates: R3, R14, H25 of finger 1; R42, S45, H53 of finger 2; and R70 and S75 of finger 3. The histidines that contact the phosphates also are ligands for the zinc ion. (The orientation of the complex is the same as in Fig. 3A.)

and O6 of the guanine at the 3′ end of the subsite. $Arg^{18}$ hydrogen bonds with the G at base pair 10, $Arg^{46}$ hydrogen bonds with the G at base pair 7, and $Arg^{74}$ hydrogen bonds with the G at base pair 4 (Fig. 3, A and B, and Fig. 5). Each of these arginine-guanine contacts is stabilized by a conserved aspartic acid that occurs as the second residue in each of the α helices. Both oxygens of the carboxylate group of the aspartic acid are in a hydrogen bond–salt bridge interaction with the Nε and Nη of the guanidinium group of the arginine (Fig. 3D). We presume that this side chain–side chain interaction helps position and stabilize the long side chain of the arginine and enhances the specificity of the arginine-guanine contacts. In addition to stabilizing the arginine, the aspartic acid at the second position in each of the α helices has one of its carboxylate oxygens within hydrogen bonding distance of a neighboring base on the secondary strand (C-rich strand) of the DNA. However, the geometry of these hydrogen bonds is not favorable, and we presume they do not play a major role in recognition.

Residue 3 is the next critical recognition residue on the α helix. In fingers 1 and 3, this position is occupied by a glutamic acid ($Glu^{21}$ and $Glu^{77}$, respectively) that does not contact the DNA. However, in finger 2 this third position is occupied by a histidine ($His^{49}$) which forms a hydrogen bond with the guanine at the middle of the subsite (Fig. 3, A, B, and F). (This histidine is not a zinc ligand—those histidines occur later in the α helix.) In our model, the Nε of $His^{49}$ donates a hydrogen bond to the N7 of the G at base pair 6, but a structure that has the His rotated 180° about the Cβ-Cγ bond and allows hydrogen bonding to the O6 of the G is equally consistent with the crystallographic data. The imidazole ring of $His^{49}$ is coplanar with the G and stacks against the T of base pair 5. The stacking seems to limit the conformational flexibility of $His^{49}$, thus enhancing the specificity of this hydrogen bonding interaction.

Residue 6 of the α helix is the last residue involved in base contacts. In fingers 1 and 3, this position is occupied by an arginine that donates a pair of charged hydrogen bonds to the N7 and O6 of the guanine at the 5′ end of the subsite (Fig. 3, A, B, and E). $Arg^{24}$ hydrogen bonds with the G at base pair 8, and $Arg^{80}$ hydrogen bonds with the G at base pair 2 (Fig. 3, A and B). Finger 2 has a threonine at this position, but $Thr^{52}$ does not seem to participate in recognition.

In summary, whenever a residue is conserved at one of the recognition positions, it makes a conserved base contact. None of the Zif268 zinc fingers contacts all three bases, but there is a relatively simple pattern to recognition: the residue immediately preceding the α helix contacts the third base on the primary strand of the subsite (5′ - - G), the third residue on the α helix can contact the second base on the primary strand (5′ - G -), and the sixth residue on the α helix can contact the first base (5′ G - -) of the 3-bp subsite.

**Contacts with the DNA backbone.** As mentioned previously, the first histidine that coordinates the zinc ion also hydrogen bonds to a phosphate on the primary strand of the DNA. This histidine, which is the seventh residue in each of the α helices, coordinates the $Zn^{2+}$ through its Nε and contacts the phosphodiester oxygens with its Nδ. This interaction is analogous to the zinc-histidine-carboxylate interaction observed in carboxypeptidase A (*32, 33*). As shown in Fig. 4, $His^{25}$ contacts the 5′ phosphate of base pair 7, and $His^{53}$ contacts the 5′ phosphate of base pair 4. These contacts are to a "neighboring subsite" and overlap a region where the next finger is contacting the bases. Because of this overlap, the phosphate that $His^{81}$ (finger 3) would contact is outside the consensus binding site, and thus absent from our DNA duplex. Nevertheless, this finger makes an analogous interaction: A water molecule bridges the Nδ of $His^{81}$ to the 5′-OH of base 1. These histidine-phosphate contacts seem remarkable for several reasons. First, the zinc makes an unexpected and direct contribution to the overall binding energy. Second, since this contact is made by an invariant histidine we

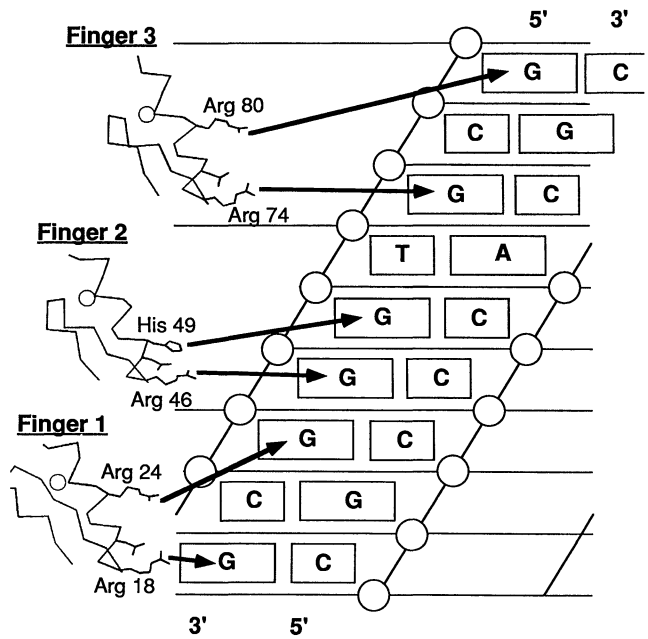


**Fig. 5.** Sketch summarizing all the base contacts made by the Zif268 peptide. The DNA is represented as a cylindrical projection.

**Table 2.** Local helical parameters for the DNA site.

| BASE PAIRS: | | HELICAL TWIST | RISE/BP | PROPELLER TWIST | TILT | ROLL |
|---|---|---|---|---|---|---|
| 2 | G : C | ----------> | | -2.235 | 12.125 | 5.016 |
| | | 24.264 | 3.484 | | | |
| 3 | C : G | ----------> | | -2.983 | 9.861 | 4.482 |
| | | 39.200 | 2.938 | | | |
| 4 | G : C | ----------> | | -6.175 | 4.099 | 3.868 |
| | | 25.534 | 3.484 | | | |
| 5 | T : A | ----------> | | -6.770 | 4.383 | 0.203 |
| | | 36.414 | 3.369 | | | |
| 6 | G : C | ----------> | | -10.329 | 0.754 | 2.490 |
| | | 31.203 | 3.266 | | | |
| 7 | G : C | ----------> | | -7.233 | 1.537 | 6.469 |
| | | 35.594 | 3.371 | | | |
| 8 | G : C | ----------> | | -11.769 | 5.805 | 11.934 |
| | | 26.571 | 3.140 | | | |
| 9 | C : G | ----------> | | -3.700 | 13.092 | 7.922 |
| | | 39.708 | 3.451 | | | |
| 10 | G : C | ----------> | | -7.413 | 13.613 | 1.032 |
| | | 29.219 | 3.177 | | | |
| 11 | T : A | ----------> | | -5.057 | 12.863 | 4.421 |
| MEAN: | | 31.967 | 3.298 | -6.366 | 7.813 | 4.784 |

expect that it is widely conserved among zinc finger–DNA complexes. Finally, this interaction uses the most central structural feature of the zinc finger—the tetrahedral geometry around the zinc ion—to orient the finger for site-specific recognition.

A conserved arginine on the second β strand also contacts phosphodiester oxygens on the primary DNA strand. In finger 1, $Arg^{14}$ contacts the 5′ phosphate of base 7; in finger 2, $Arg^{42}$ contacts the 5′ phosphate of base 5; and, in finger 3, $Arg^{70}$ contacts the 5′ phosphate of base 2. Fingers 2 and 3 contact equivalent phosphates (with respect to the 3-bp subsites), whereas the finger 1 contact is shifted by one nucleotide.

In addition to the conserved histidine and arginine contacts made by each finger, the Zif268 peptide makes four other phosphate contacts. $Arg^{3}$, which precedes finger 1, contacts the 5′ phosphate of base 8 on the primary DNA strand, and $Arg^{87}$ contacts a phosphate on the primary strand of a symmetry-related DNA molecule. $Ser^{45}$ (finger 2) hydrogen bonds to the 5′ phosphate of base 6 on the primary strand, and $Ser^{75}$ (finger 3) hydrogen bonds to the phosphate between base pairs 7 and 8 on the secondary strand. The $Ser^{75}$ contact is the only backbone contact that the zinc finger makes with the secondary strand of the DNA.

**Structure of the zinc finger**. The overall structures of the three fingers are similar, and superimposing them gives excellent alignment of the corresponding residues (Fig. 6A). The α carbons of fingers 2 and 3 (residues 34 to 57 and 62 to 85) can be superimposed with a rms deviation of 0.45 Å. Finger 1 (excluding the two extra residues in the loop between the two cysteines of this finger) can be superimposed on finger 2, or on finger 3, with rms deviations of 0.83 Å and 0.87 Å, respectively. The NMR structure of Xfin31 (*18*) aligns best with finger 2 (residues 35–57) with an rms deviation of 0.74 Å. Since all three fingers have essentially the same secondary structures, we describe only the structure of finger 1 (Fig. 6B) and note significant differences as they occur.

$Pro^{4}$ is the first zinc finger consensus residue of finger 1, and it has van der Waals contacts with the side chain of $Tyr^{5}$, which is a highly conserved aromatic residue. This proline-aromatic interaction is conserved in fingers 2 and 3, and it may play an important role in restricting the conformation of the polypeptide chain at the start of the zinc finger.

The polypeptide chain then forms a hairpin with an antiparallel β-sheet stem and a turn near the conserved cysteines. This region encompasses residues 5 to 16 of finger 1. The antiparallel β sheet has three backbone hydrogen bonds: the first one is between $Tyr^{5}$-NH and $Phe^{16}$-CO, the second one is between $Tyr^{5}$-CO and $Phe^{16}$-NH, and the third one is between $Cys^{7}$-NH and $Arg^{14}$-CO. The φ-ψ angles in this region are typical of an antiparallel β sheet. In finger 1, the turn between these two β strands contains residues 8 to 13. In this turn, residues 9, 10, and 11 appear to be flexible and are poorly defined in our electron density maps. Fingers 2 and 3 have a shorter loop (two residues between the cysteines) and the turns in these fingers have well-defined conformations. Each of these fingers has a pair of conserved hydrogen bonds from backbone amides to the sulfhydryl of the first cysteine. In finger 2, $Ile^{39}$-NH and $Cys^{40}$-NH

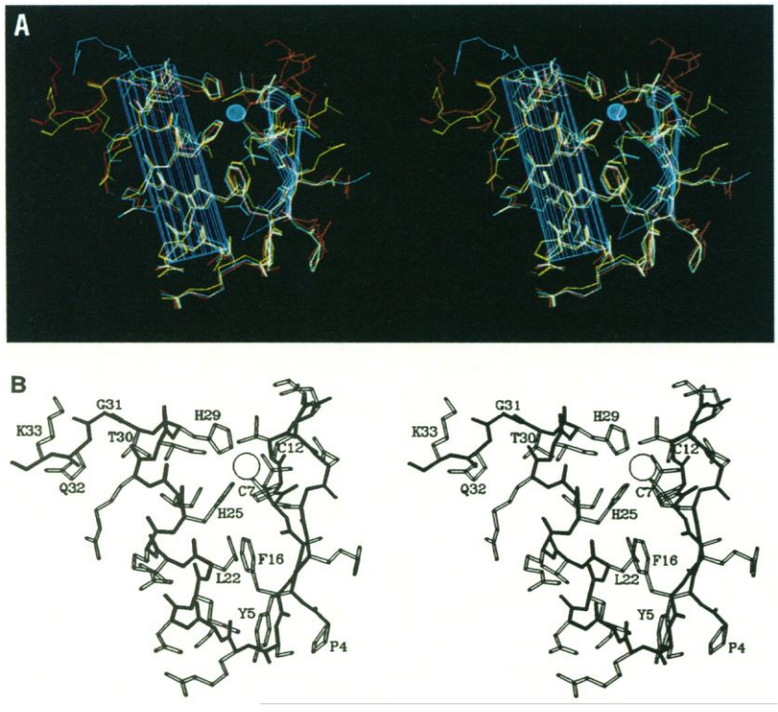


**Fig. 6.** The structure of the zinc finger. (**A**) The overall structures of the three fingers are essentially the same. Stereo photograph showing the three fingers superimposed (via their Cα's). The light blue cylinder and ribbon indicate the secondary structure of finger 2. Finger 1 is red, finger 2 is yellow, and finger 3 is blue. (**B**) Stereo diagram of finger 1 (residues 4 to 33) in a view similar to that of Fig. 6A. The conserved hydrophobic residues (P4, Y5, F16, L22), the four residues that coordinate the zinc ion (C7, C12, H25, H29), and the linker residues (T30, G31, Q32, K33) are labeled.

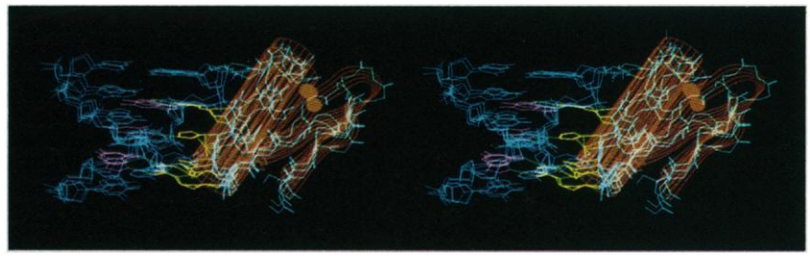

**Fig. 7.** Each of the three fingers binds DNA in a similar orientation. The subsites of the three fingers were superimposed by aligning the phosphates of the DNA backbone. Although the protein was not used in the alignment, the fingers and the conserved contacts superimposed very well. The DNA and the fingers are shown in blue, the secondary structures of each finger are indicated with orange cylinders and ribbons, the side chains that contact the bases are shown in yellow, and the bases that are contacted are shown in purple.

hydrogen bond with the $Cys^{37}$-Sγ, and in finger 3, $Ile^{67}$-NH and $Cys^{68}$-NH hydrogen bond with the $Cys^{65}$-Sγ.

Only two residues are required to make the transition from the β sheet to the α helix. In finger 1, $Ser^{17}$ and $Arg^{18}$ connect these secondary structures. Although the backbone carbonyl of $Arg^{18}$ makes the first α-helical hydrogen bond with the backbone amide of $Leu^{22}$, the backbone of $Arg^{18}$ is not in an α-helical conformation. The regular α helix begins with $Ser^{19}$ and continues for several residues. A kink occurs near the center of the helix, and the kink is followed by several hydrogen bonds characteristic of a $3_{10}$ helical arrangement. Specifically, the kink occurs because $Thr^{23}$-CO and $Arg^{24}$-CO are too far away from their normal hydrogen bond partners (4.0 Å and 4.7 Å, respectively). The backbone carbonyl of $His^{25}$ hydrogen bonds with the $Ile^{28}$-NH in a $3_{10}$ helical arrangement, and $Ile^{26}$-CO makes a bifurcated hydrogen bond to both $His^{29}$-NH (as expected for a $3_{10}$ helix) and to $Thr^{30}$-NH (as expected for an α helix). This allows for a smooth transition back to a regular α helix. The next, and last, α-helical bond is between $Arg^{27}$-CO and $Gly^{31}$-NH. $Gly^{31}$ has nonhelical φ-ψ angles and essentially terminates the α helix. Overall, the kink bends the second half of the α helix toward the zinc binding site and thus puts the second histidine in a position where it can coordinate the metal. The same kink (involving an identical hydrogen bonding pattern) is also observed in fingers 2 and 3.

In addition to the zinc ion, each finger also is stabilized by a hydrophobic core involving the highly conserved Phe (which is residue 16 in finger 1), Leu (residue 22), and His (residue 25). This core also involves a number of moderately conserved hydrophobic residues ($Val^{9}$, $Ile^{26}$, $Ile^{28}$, and $Thr^{30}$ in finger 1) which form hydrophobic patches on both sides of the finger and help shield the zinc binding site from the solvent.

The sequence Thr-Gly-Glu-Lys has been called the "linker" [or H-C link (*34*)] since it occurs between fingers and since this sequence is conserved in a large number of zinc finger proteins. In the Zif268 peptide, the linker between fingers 1 and 2 (Thr-Gly-Gln-Lys) deviates slightly from the consensus, whereas the linker between fingers 2 and 3 exactly matches the consensus sequence. Our cocrystal structure shows that the first linker residue, $Thr^{30}$, is actually in the α helix of the zinc finger. As mentioned earlier, its methyl group is involved in hydrophobic interactions on one side of the finger. In addition, the -OH of this threonine hydrogen bonds to the backbone amide of the third linker residue ($Gln^{32}$). The second linker residue, $Gly^{31}$, makes the last hydrogen bond of the α helix and seems to play an important role in terminating the α helix. In our maps, the side chains for the third and fourth linker residues ($Gln^{32}$ and $Lys^{33}$) have weaker electron density, and they do not seem to have any important contacts with the rest of the protein or with the DNA. Both of the linkers in our cocrystal structure have the same well-defined backbone conformations, and they probably play an important role in controlling the orientation and spacing of adjacent fingers.

There are not many contacts between the fingers, but the side chain of the conserved $Arg^{27}$ hydrogen bonds to the backbone carbonyl of $Ser^{45}$, which is in the turn between the β sheet and the α helix of the next finger. The same interaction is also observed between fingers 2 and 3, where $Arg^{55}$ hydrogen bonds to the backbone carbonyl of $Ala^{73}$.

**Structure of the DNA.** There has been considerable speculation that zinc fingers may bind to A-DNA or to some very distinct form of B-DNA. However, we find that the 11-bp DNA in the cocrystal is essentially a B-type helix. The average rise per base pair is 3.3 Å (Table 2), which is very close to the 3.4 Å rise expected for B-DNA. The average helical twist of 32.0° (11.3 bp per turn) is a few degrees smaller than that expected for B-DNA (*35*) (34.3°, which corresponds to 10.5 bp per turn). This small difference could result from crystal packing forces since the 11-bp DNA duplexes stack end-to-end to form a pseudo-continuous helix, and thus the DNA is constrained to have an 11-bp repeat. Although the overall structure clearly is characteristic of B-DNA, the subsites for fingers 1 and 3 show considerable internal variations in their base pair twists. The helical twist between base pairs 2 and 3 is 24.3°, and the helical twist between base pairs 3 and 4 is 39.2° (Table 2). A corresponding arrangement is found in the other subsite. The helical twist between base pairs 8 and 9 is 26.6°, and the twist between base pairs 9 and 10 is 39.7°. These deviations in helical twists among neighboring base pairs tend to cancel each other, resulting in overall twists for subsites 1 and 3 that are very close to the average. Within each subsite however, these twists cause the positions of the bases C3 and C9 to be substantially different from what they would have been in an idealized B-DNA helix.

**Comparison of the orientations of the three fingers.** Each of the three fingers binds in a similar orientation and makes similar contacts with 3 bp of the DNA. This conserved spatial relation implies that each finger is related to the next by a simple helical motion. Formally speaking, this combination of a rotation and a translation is a "screw" motion. Rotating by about 96° (three times the average helical twist per base pair) and translating by about 10 Å (three times the average rise per base pair) will superimpose one finger on the next. This structure is consistent with the model for zinc finger binding in the major groove, which was favored by Berg (*36, 37*) after modeling the zinc finger domain. It is inconsistent with the model that has alternate fingers in rather different orientations (*38*).

The conserved spatial relation can be illustrated by dissecting the complex into three subsites (with a single finger bound to each) and then superimposing the DNA backbone for each subsite. The three fingers superimpose extremely well, even though the protein structure was not used when aligning the subsites (Fig. 7). This demonstrates that the three fingers of the Zif complex have very similar orientations with respect to the DNA. This conserved spatial arrangement is consistent with our observation that the three-fingers contact the DNA with a similar set of residues and that they make a closely related set of side chain–base interactions. It appears that this orientation is ideal for the arginine-guanine contacts that are so critical for the Zif268 zinc fingers. However, it is possible that a somewhat different arrangement would be needed with shorter side chains, and it will be interesting to see how many different zinc finger–DNA relationships are found in other complexes.

**Implications for understanding protein-DNA interactions.** This structure reemphasizes the central role that α helices have in site-specific recognition. Previous crystallographic studies of protein-DNA complexes had shown how helices are used by the prokaryotic helix-turn-helix proteins (*39–41*) and by the eukaryotic homeodomain (*42*); our work now proves that helices are used by another major family of DNA-binding proteins—zinc fingers. NMR studies of the steroid receptor DNA-binding domain (*14*) and circular dichroism studies of the basic region of leucine zipper peptides (*43*) suggest that these proteins also use helices for site-specific recognition. Although extended secondary structures, such as the $NH_2$-terminal arms of λ repressor and *Engrailed*, and β sheets, as in the prokaryotic MetJ repressor (*44*), can also have a major role in protein-DNA recognition, it now appears that the major families of DNA-binding proteins use α-helical regions to make the critical contacts with the bases.

Although Zif268 also uses α helices for recognition, the Zif complex is significantly different from previously characterized complexes. Several features of the Zif complex are distinctive.

1) Unlike the helix-turn-helix proteins, this zinc finger complex is based on modular units (individual fingers) which are repeated in a way that allows each finger to contact 3 bp. This appears to be the first clear instance where the periodicity of the protein structure is a simple function of the periodicity of the double-helical DNA. Recognition is based on a modular system that can be used to recognize extended, asymmetric sites.

2) The majority of the contacts are made with a single strand of the DNA.

3) Recognition appears to rely heavily on base contacts in the zinc finger–DNA complex. There are fewer hydrogen bonds with the DNA backbone and they generally appear to play a less critical role in orienting the protein (although the phosphate contact made by the histidine ligand may be quite important). Base contacts appear to play a greater role in orienting the fingers. Since these may change from one complex to the next, it is possible that this makes the zinc finger more "adaptable" than other motifs.

4) Although studies of other protein-DNA complexes have suggested that there is no recognition code, arginine-guanine contacts seem to be very important for the Zif complex.

In spite of these important differences, the Zif complex shows some broad similarities with the prokaryotic helix-turn-helix proteins and with the eukaryotic homeodomain. In some sense, it appears that the finger structure just provides another mechanism for getting an α helix into the major groove, and the critical role of the α-helical regions tends to unite the major families of DNA-binding proteins. As observed in the prokaryotic helix-turn-helix proteins and the eukaryotic homeodomain, other parts of the conserved structural motif contact the DNA backbone and help to precisely position the helix within the major groove. These contacts may have similar functional roles even though Zif268 uses a β strand to contact the DNA backbone while the λ repressor and the Engrailed homeodomain use the first helix of the helix-turn-helix unit to make the corresponding contacts. In each case these neighboring regions may serve as an "outrigger" that keeps the helix from rolling in the major groove. Although the Zif complex has fewer contacts with the DNA backbone, the total number of hydrogen bonds between the protein and the DNA is comparable to that reported with other protein-DNA complexes. As noted in the λ repressor-operator complex, side chain–side chain interactions are important for site-specific recognition (*39*). Finally, most of the major groove contacts in other complexes also involve purines. This may occur simply because the purines occupy a greater portion of the major groove and offer more hydrogen bonding sites than the pyrimidines. However, it is possible that having a pair of hydrogen bonds (instead of a single hydrogen bond with a pyrimidine) with a rigid planar structure may give enhanced specificity in recognition.

**Conclusions.** The structure of the Zif complex reveals a remarkably simple and efficient mechanism for recognizing specific sites on double-stranded DNA. The α helix of each zinc finger fits directly into the major groove of B-DNA, and side chains from the $NH_2$-terminal portion of this helix contact the edges of the base pairs. The main contacts from each finger involve a 3-bp subsite. The Zif268 zinc fingers are tandemly arranged in the major groove, and thus the three finger peptide contacts a 9-bp site. Most of the contacts are along one strand of the DNA (the G-rich strand) and the peptide is "antiparallel" to the DNA strand that has the primary contacts. Arginine-guanine contacts, similar to those discussed by Seeman, Rosenberg, and Rich (*45*), appear to be responsible for much of the specificity in the Zif complex. There are relatively few contacts with the backbone of the DNA, but one of these contacts is made by a histidine that also serves as a zinc ligand. The second β strand of each finger is near the sugar phosphate backbone of the DNA, and an arginine from this strand also makes a conserved contact with a phosphodiester oxygen.

The structure of the Zif complex should provide a useful guide for modeling complexes with closely related fingers, such as Sp1 (*9*), and it also provides an attractive framework for attempts to design DNA-binding proteins with novel specificities. Since each finger makes its primary contacts along a 3-bp region, it might be possible to design (or find) fingers that would recognize each of the 64 possible base pair triplets. Then one could "mix and match" these fingers to design proteins with any desired sequence specificity. The main issues involved in modeling homologous fingers and in designing new fingers are similar. We need to find out how fingers are arranged in other complexes and how fingers can be used to recognize other sequences. It is possible that zinc fingers (even fingers of the TFIIIA subclass) may be used in different ways in different complexes. Comparing the homeodomain-DNA complex with the λ repressor–operator complex showed that the helix-turn-helix unit can be used in rather different ways (*42*), and fingers are so common that evolution will have had a chance to explore all possible ways of using them. It will be necessary to solve the structures of several other zinc finger–DNA complexes to determine whether this overall arrangement is conserved and to see the precise contacts made by fingers that recognize A-T–rich sites.

REFERENCES AND NOTES


1. J. Miller, A. D. McLachlan, A. Klug, *EMBO J.* **4**, 1609 (1985).
2. G. Jacobs and G. Michaels, *New Biol.* **2**, 583 (1990).
3. V. P. Sukhatme *et al.*, *Cell* **53**, 37 (1988).
4. B. A. Christy, L. F. Lau, D. Nathans, *Proc. Natl. Acad. Sci. U.S.A.* **85**, 7857 (1988).
5. L. J. Joseph *et al.*, *ibid.*, p. 7164.
6. P. Chavrier *et al.*, *EMBO J.* 7, 29 (1988).
7. K. W. Kinzler, J. M. Ruppert, S. H. Bigner, B. Vogelstein, *Nature* **332**, 371 (1988).
8. K. M. Call *et al.*, *Cell* **60**, 509 (1990).
9. D. Gidoni, S. W. Dynan, R. Tjian, *Nature* **312**, 409 (1984).
10. D. Tautz *et al.*, *ibid.* **327**, 383 (1987).
11. U. B. Rosenberg *et al.*, *ibid.* **319**, 336 (1986).
12. L. T. Bemis and C. L. Denis, *Mol. Cell. Biol.* **8**, 2125 (1988).
13. T. H. Adams, M. T. Boylan, W. E. Timberlake, *Cell* **54**, 353 (1988).
14. T. Härd *et al.*, *Science* **249**, 157 (1990).
15. T. Pan and J. E. Coleman, *Proc. Natl. Acad. Sci. U.S.A.* **87**, 2077 (1990).
16. M. F. Summers, T. L. South, B. Kim, D. R. Hare, *Biochemistry* **29**, 329 (1990).
17. G. Párraga *et al.*, *Science* **241**, 1489 (1988).
18. M. S. Lee, G. P. Gippert, K. V. Soman, D. A. Case, P. E. Wright, *ibid.* **245**, 635 (1989).
19. J. Nardelli, T. J. Gibson, C. Vesque, P. Charnay, *Nature* **349**, 175 (1991).
20. B. Christy and D. Nathans, *Proc. Natl. Acad. Sci. U.S.A.* **86**, 8737 (1989).
21. F. W. Studier, A. H. Rosenberg, J. J. Dunn, J. W. Dubendorff, *Methods Enzymol.* **185**, 60 (1990).
22. N. P. Pavletich and C. O. Pabo, unpublished data.
23. S.E.R.C. [U.K.] Collaborative Computing Project No. 4 (Daresbury Laboratory,

Warrington, U.K., 1979).
24. B. C. Wang, *Methods Enzymol.* **115**, 90 (1985).
25. M. A. Rould, J. J. Perona, D. Söll, T. A. Steitz, *Science* **246**, 1135 (1989).
26. T. A. Jones, *J. Appl. Cryst.* **11**, 268 (1978).
27. A. T. Brünger, J. Kuriyan, M. Karplus, *Science* **235**, 458 (1987).
28. A. T. Brünger, *X-PLOR v2.1 Manual* (Yale Univ. Press, New Haven, CT, 1990).
29. D. E. Tonrud, L. F. Ten Eyck, B. W. Matthews, *Acta Crystallogr.* **A43**, 489 (1987).
30. D. R. Smith, I. J. Jackson, D. D. Brown, *Cell* **37**, 645 (1984).
31. K. E. Vrana, M. E. A. Churchill, T. D. Tullius, D. D. Brown, *Mol. Cell. Biol.* **8**, 1684 (1988).
32. D. C. Rees, M. Lewis, W. N. Lipscomb, *J. Mol. Biol.* **168**, 367 (1983).
33. D. W. Christianson and R. S. Alexander, *J. Am. Chem. Soc.* **111**, 6412 (1989).
34. R. Schuh *et al.*, *Cell* **47**, 1025 (1986).
35. J. C. Wang, *Proc. Natl. Acad. Sci. U.S.A.* **76**, 200 (1979).
36. J. M. Berg, *ibid.* **85**, 99 (1988).
37. ———, *J. Biol. Chem.* **265**, 6513 (1990).
38. L. Fairall, D. Rhodes, A. Klug, *J. Mol. Biol.* **192**, 577 (1986).
39. S. R. Jordan and C. O. Pabo, *Science* **242**, 893 (1988).
40. A. K. Aggarwal, D. W. Rodgers, M. Drottar, M. Ptashne, S. C. Harrison, *ibid.* p. 899.
41. Z. Otwinowski *et al.*, *Nature* **335**, 321 (1988).
42. C. R. Kissinger, B. Liu, E. Martin-Blanco, T. B. Kornberg, C. O. Pabo, *Cell* **63**, 579 (1990).
43. K. T. O'Neil, R. H. Hoess, W. F. DeGrado, *ibid.* **249**, 774 (1990).
44. J. B. Rafferty, W. S. Somers, I. Saint-Girons, S. E. V. Phillips, *Nature* **341**, 705 (1989).
45. N. C. Seeman, J. M. Rosenberg, A. Rich, *Proc. Natl. Acad. Sci. U.S.A.* **73**, 804 (1976).
46. Supported by NIH grant GM-31471 (C.O.P.) and by the Howard Hughes Medical Institute. We thank B. Christy and D. Nathans for providing us with the cDNA clone of *zif268* and the sequence of the Zif268 binding site; P. Wright for providing us with the coordinates of the NMR structure of Xfin31; E. M. Westbrook and M. L. Westbrook for the use of the Midwest Area Detector User Facility; A. Collector and C. Wendling for synthesizing the DNA; U. Obeysekare for writing some of the graphics subroutines; the members of the Pabo laboratory, especially C. R. Kissinger, for help with the structure determination; and the National Cancer Institute for use of the Cray during molecular dynamics refinement. Coordinates are being deposited with the Brookhaven Data Bank. While these are being processed by Brookhaven and prepared for distribution, interested scientists may obtain a set of coordinates either by sending an appropriate BITNET address to us at PABO@JHUIGF or by sending a 1/2-inch tape with a mailing envelope and sufficient return postage.

13 February 1991; accepted 19 March 1991

# A New Cofactor in a Prokaryotic Enzyme: Tryptophan Tryptophylquinone as the Redox Prosthetic Group in Methylamine Dehydrogenase

WILLIAM S. MCINTIRE,* DAVID E. WEMMER, ANDREI CHISTOSERDOV, MARY E. LIDSTROM

**Methylamine dehydrogenase (MADH), an $\alpha_2\beta_2$ enzyme from numerous methylotrophic soil bacteria, contains a novel quinonoid redox prosthetic group that is covalently bound to its small β subunit through two amino acyl residues. A comparison of the amino acid sequence deduced from the gene sequence of the small subunit for the enzyme from *Methylobacterium extorquens* AM1 with the published amino acid sequence obtained by the Edman degradation method, allowed the identification of the amino acyl constituents of the cofactor as two tryptophyl residues. This information was crucial for interpreting $^1H$ and $^{13}C$ nuclear magnetic reasonance, and mass spectral data collected for the semicarbazide- and carboxymethyl-derivatized bis(tripeptidyl)-cofactor of MADH from bacterium W3A1. The cofactor is composed of two cross-linked tryptophyl residues. Although there are many possible isomers, only one is consistent with all the data: The first tryptophyl residue in the peptide sequence exists as an indole-6,7-dione, and is attached at its 4 position to the 2 position of the second, otherwise unmodified, indole side group. Contrary to earlier reports, the cofactor of MADH is not 2,7,9-tricarboxypyrroloquinoline quinone (PQQ), a derivative thereof, or pro-PQQ. This appears to be the only example of two cross-linked, modified amino acyl residues having a functional role in the active site of an enzyme, in the absence of other cofactors or metal ions.**

SINCE THE ELUCIDATION OF THE STRUCTURE OF THE REDOX cofactor of methanol dehydrogenase from *Pseudomonas* TP1 as 2,7,9-tricarboxy-1*H*-pyrrolo[2,3-*f*]-quinoline-4,5-dione (Fig. 1, **1**) (*1*), this quinone has been shown to be the noncovalently bound redox cofactor of several other bacterial enzymes (*2*). This prosthetic group was originally given the common name methoxatin, but, the more descriptive name pyrroloquinoline quinone (PQQ) has come into favor. More properly, this form should be called 2,7,9-tricarboxy-PQQ to distinguish it from other derivatives that may exist in nature.

A number of enzymes have been proposed to contain covalently bound PQQ or a PQQ derivative. In this group are the copper-containing amine oxidases: plasma amine oxidase, kidney, and placental diamine oxidase, lysyl oxidase, plant diamine oxidase, fungal amine oxidase, and methylamine oxidase from the soil

W. S. McIntire is in the Molecular Biology Division, Department of Veterans Affairs Medical Center, San Francisco, CA 94121, and in the Department of Biochemistry and Biophysics and the Department of Anesthesia, University of California, San Francisco, CA 94143. D. E. Wemmer is in the Department of Chemistry, University of California, Berkeley, CA 94720. A. Chistoserdov and M. E. Lidstrom are with the W. M. Keck Laboratories, California Institute of Technology, Pasadena, CA 91125.

*To whom correspondence should be addressed.